

DNA repair pathway

Catherine E. Gleason¹, Ranya Odeh¹, Frances Hamkins-Indik¹, Roberta Sala¹, Iolanda Vendrell², Roman Fischer², Benedikt Kessler², Shilpa Singh³, Matthew G. Oser³, Marie Evangelista¹, and Pablo D. Garcia¹
¹Circle Pharma, South San Francisco, CA; ²Target Discovery Institute, Nuffield Department of Medicine, University of Oxford, UK & ³Department of Medical Oncology, Dana-Farber Cancer Institute, Harvard Medical School, Boston, MA.

BACKGROUND

- Cyclins A and B are key cell cycle regulators that bind and activate their cyclin-dependent kinase (CDK) partners to regulate progression through S and G₂/M phases. Cyclins contain a highly conserved MRAIL motif forming the hydrophobic patch that facilitates interaction with a subset of Cyclin/CDK targets containing RxL (Cy) motifs.
- We generated cell-permeable, orally bioavailable macrocycles that selectively bind the hydrophobic patch of Cyclin A and B (Cyclin A/B RxLi) (Figure 1A). Cyclin A/B RxLi inhibitors achieve at least two key effects in cancer cells (Figure 1B): 1) disruption of the Cyclin A: E2F interaction that dampens E2F activity and 2) displacement of the negative regulator Myt1 from Cyclin B.
- Selectively in cancers with high E2F expression, such as small cell lung cancer (SCLC), Cyclin A/B RxL inhibitors increase E2F activity and activate Cyclin B/CDK, leading to enhanced DNA damage, spindle assembly checkpoint (SAC) activation and mitotic cell death *in vitro* and tumor regressions *in vivo* (Figures 1B and 2). A manuscript describing Cyclin A/B RxL inhibitor mechanism of action is available on BioRxiv and is currently under peer review (see reference 1).
- Here we report results using the Cyclin A/B RxLi tool compound, CIRc-004, that furthers our understanding of how disruption of RxL-dependent Cyclin A interactions may contribute to increased replication stress and unrepaired DNA damage providing new insights on the molecular therapeutic mechanism for cell death induced by Cyclin A/B RxL inhibitors.

FIGURE 1

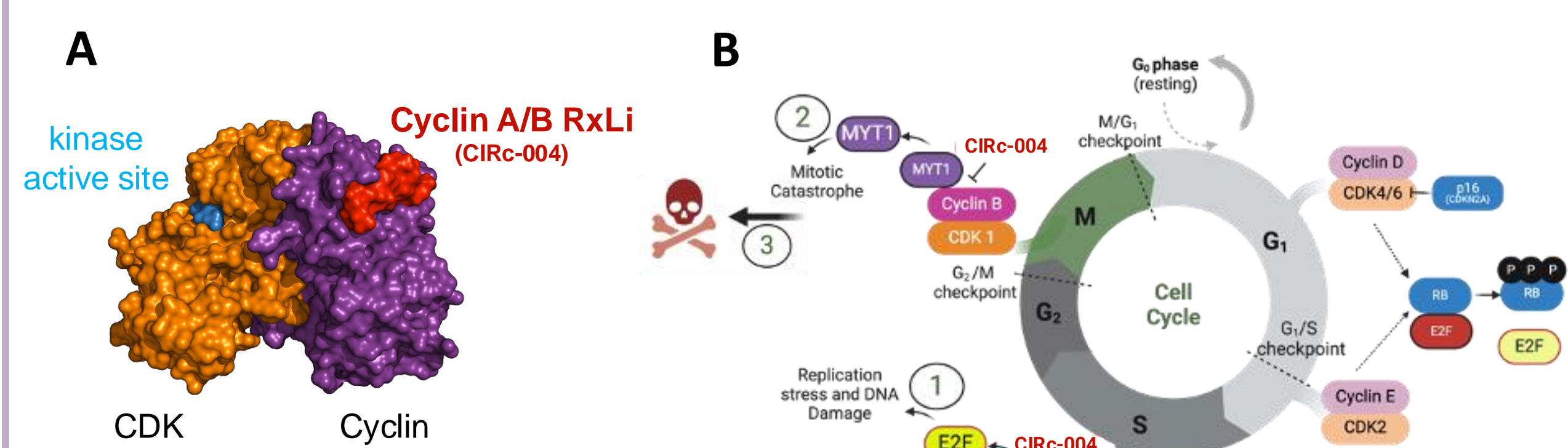
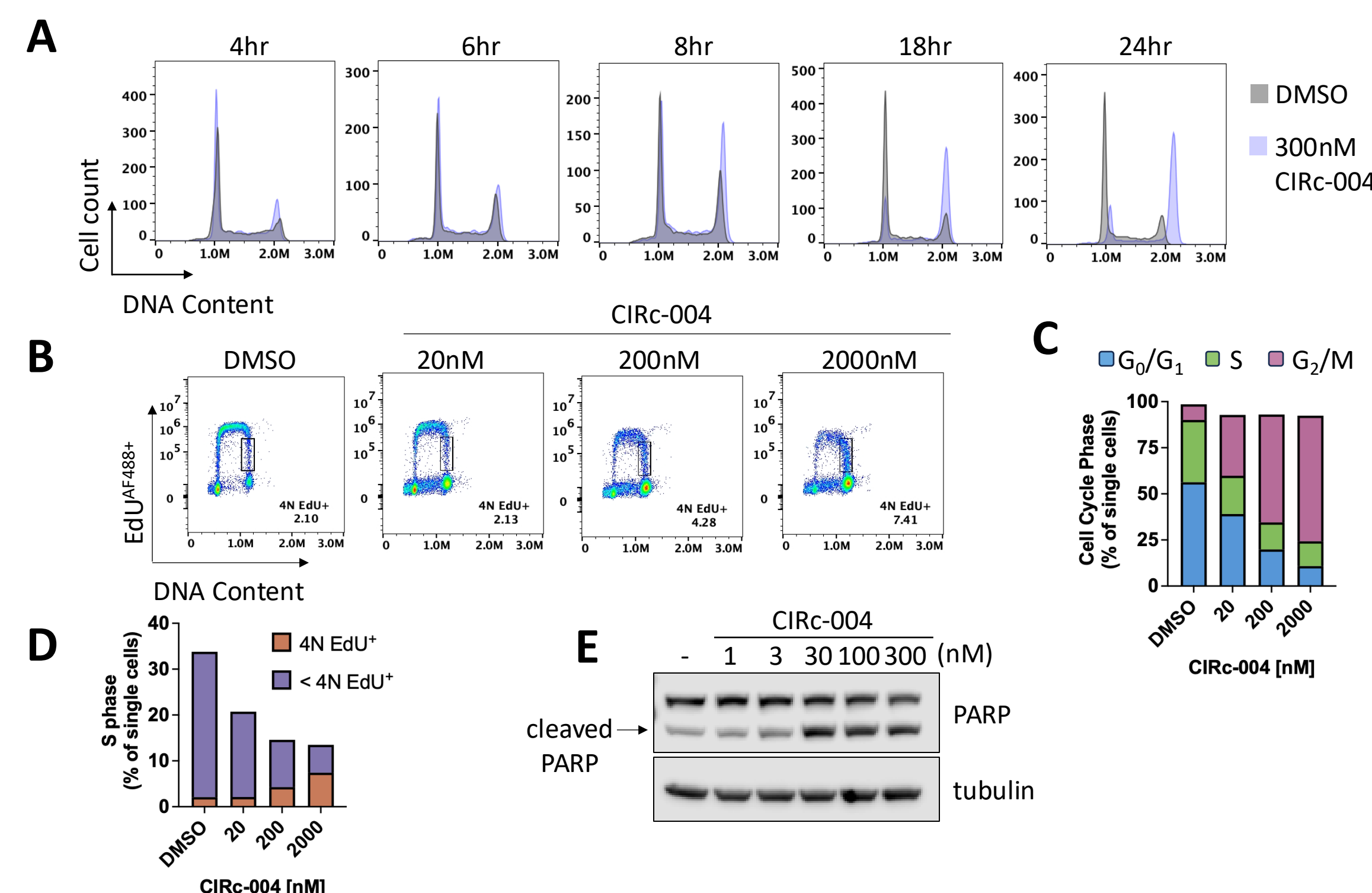


FIGURE 2. Cyclin A/B RxL inhibitors induce markers of DNA damage, mitotic accumulation and apoptosis



(A) G₂/M accumulation is observed following > 6hr exposure to Cyclin A/B RxLi. Asynchronous NCI-H1048 SCLC cells were incubated with DMSO or CIRc-004 for the indicated times before collecting for flow cytometry. DNA content was assessed by FxCycle Violet. (B, C, D) Cyclin A/B RxL inhibition results in increased EdU⁺ 4N DNA content cells, an indication of DNA damage/repair in G₂/M phase. NCI-H1048 cells were incubated with DMSO or CIRc-004 for 24hr. During the last hour, cells were pulsed with EdU before collecting for flow cytometry. (E) EdU⁺ 4N DNA content was assessed by detection of EdU⁺ 4N DNA content (FxCycle) (the box indicates the gate used to measure 4N EdU⁺ cells, the percent of single cells is indicated in the lower right corner of the plot), (C) quantification of the effect of CIRc-004 on cell cycle progression, (D) quantification of DNA replication in cells with <4N and 4N DNA content. (E) Cyclin A/B RxLi induces a dose-dependent increase in apoptosis. NCI-H1048 cells were treated for 24h with DMSO or CIRc-004 at the indicated concentrations. The induction of cleaved PARP, a marker for apoptosis, was measured by Western blot. Tubulin, loading control.

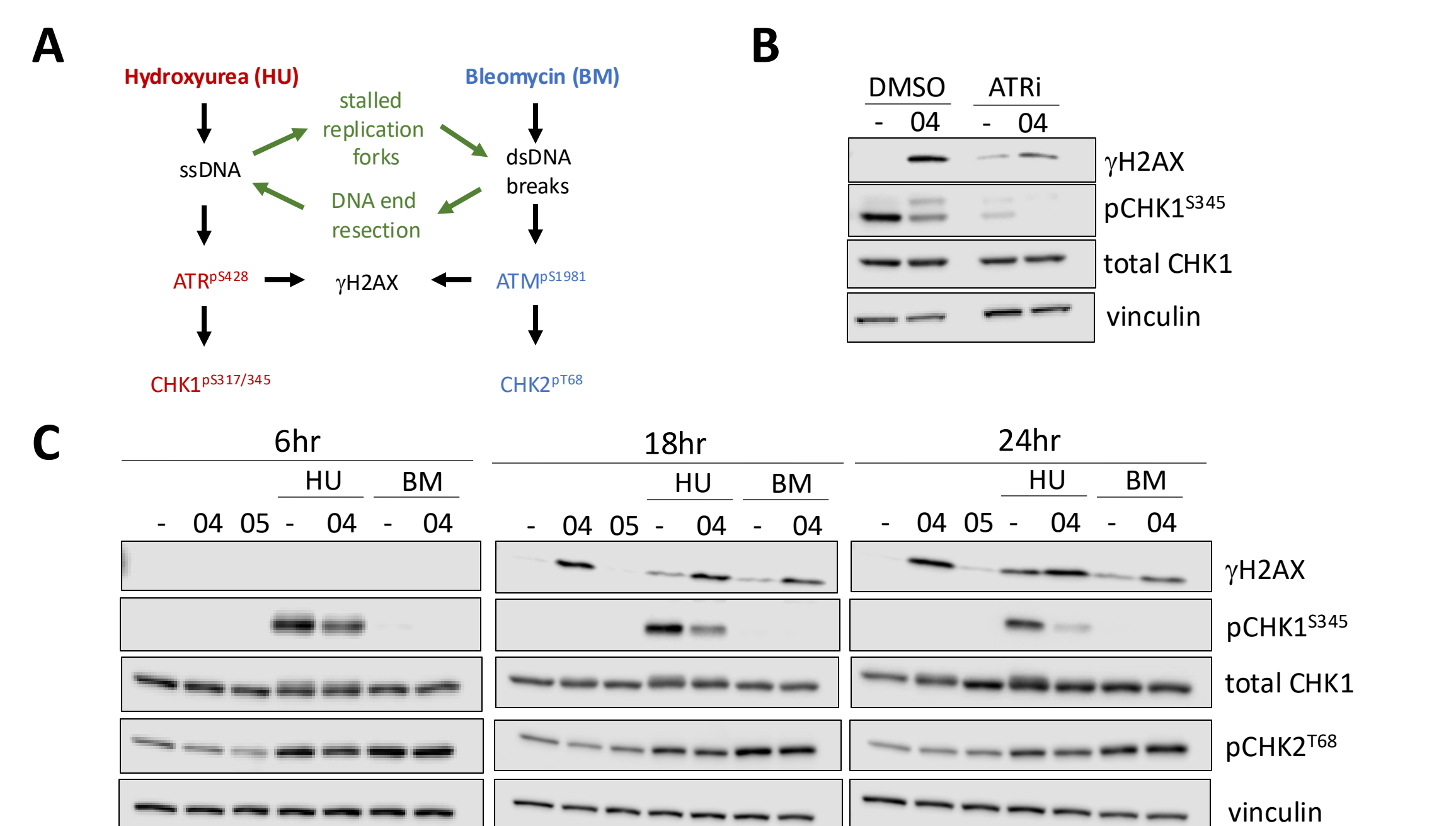
RESULTS

FIGURE 3. Biochemical potency and cell activity of Cyclin RxL inhibitor tool compounds

Compound	RxL inhibitor selectivity	Biochemical Activity			Cell Activity
		Binding Affinity (nM) ^b	GI ₅₀ (μM) ^c		
		Cyclin A	Cyclin E	Cyclin B	NCI-H1048
CIRc-004	Cyclin A/B RxL	13	260	2.0	0.032
CIRc-005	Cyclin A/B I.E ^o	NA	NA	NA	12.8
CIRc-018	Cyclin A RxL	3.1	96	137	2.43
CIRc-019	Cyclin B RxL	55	590	8.8	2.81

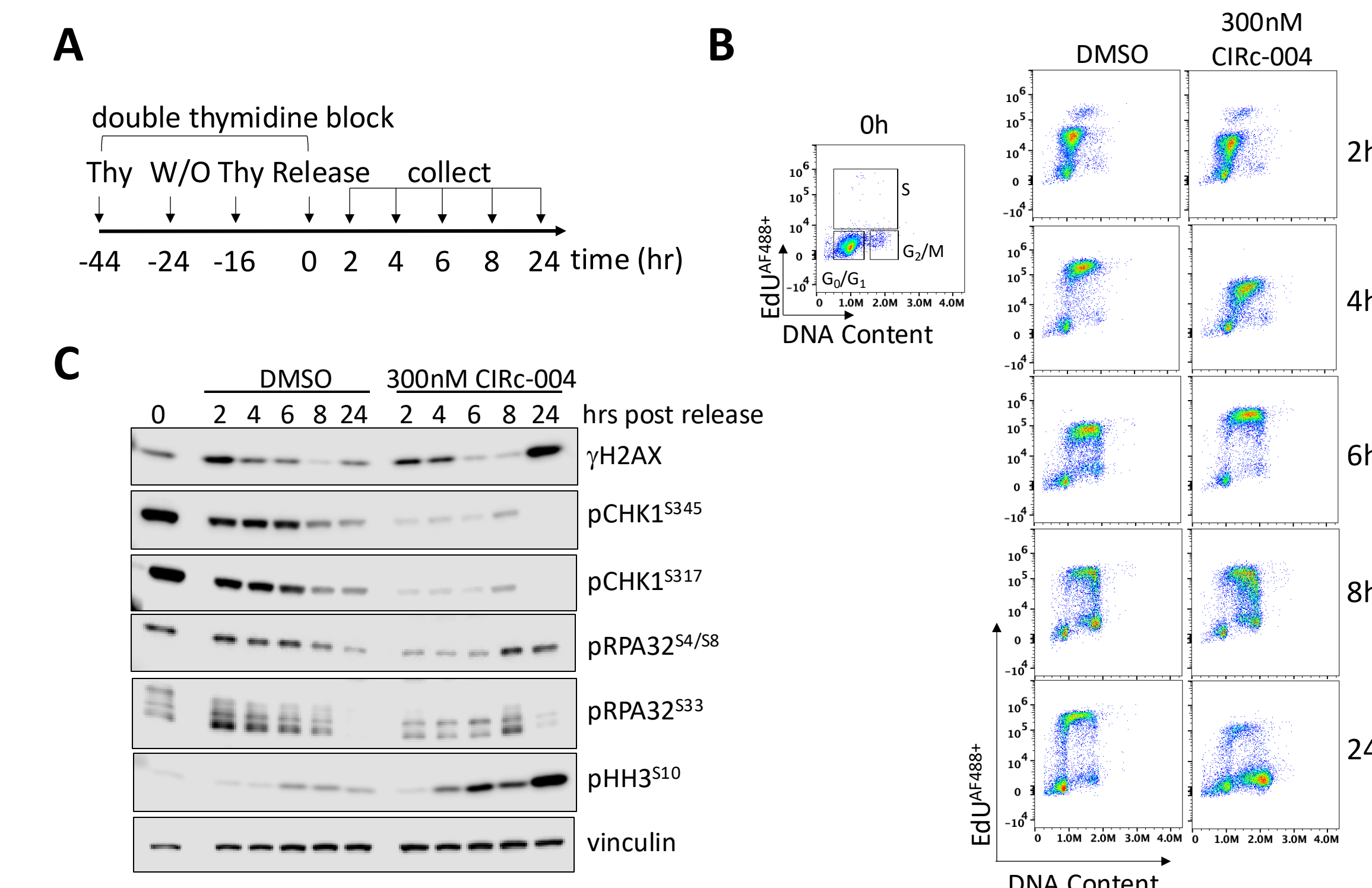
a. inactive enantiomer of CIRc-004, b. SPR, c. MTT cell proliferation assay

FIGURE 4. Cyclin A/B RxL inhibition impairs activation of the ssDNA damage repair pathway



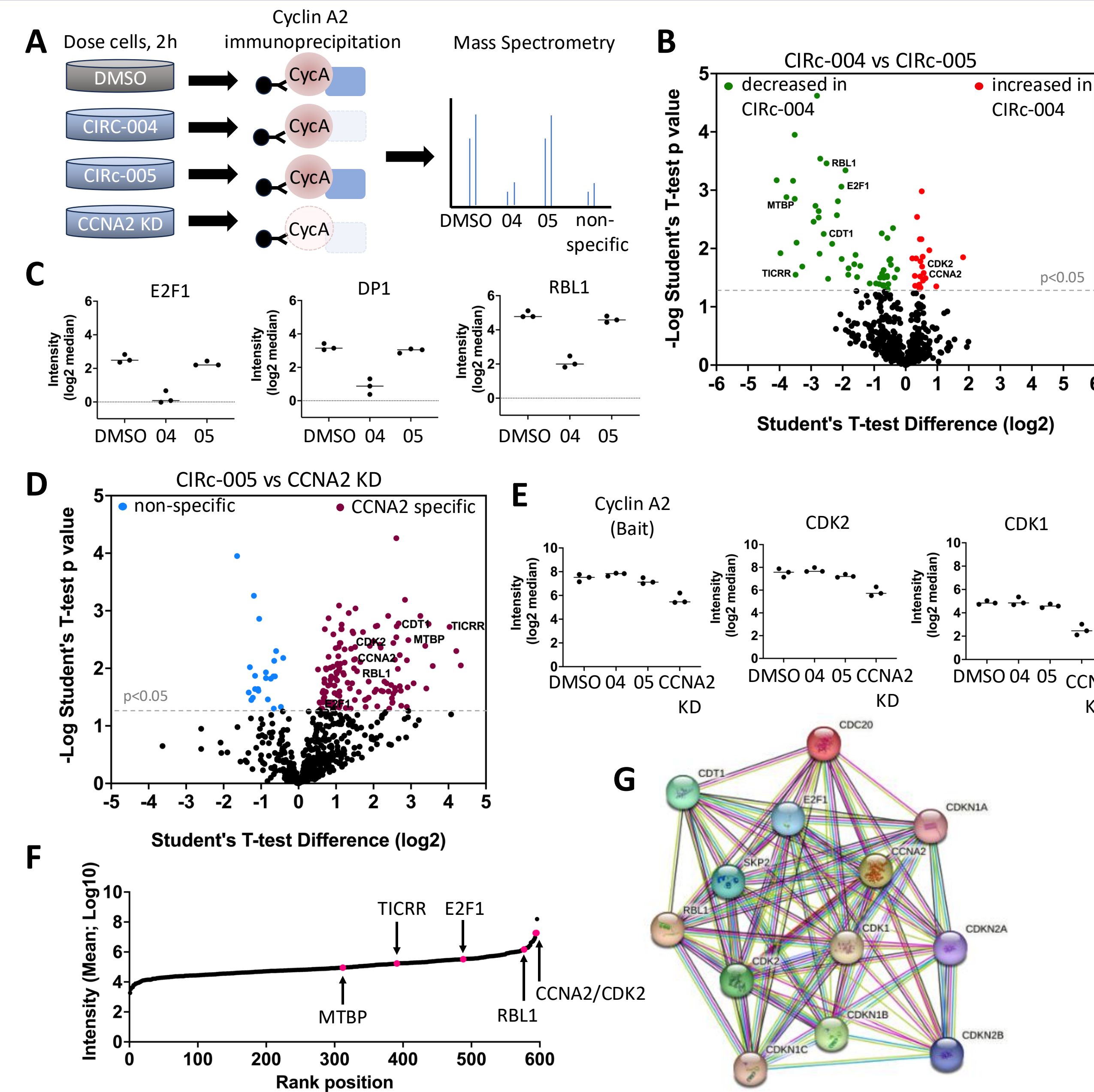
(A) Model for activation of the single strand DNA (ssDNA) and double strand DNA break (dsDNA) damage response/repair pathways. (B) Cyclin A/B RxL inhibition impairs ATR-dependent CHK1 phosphorylation while increasing the DNA damage marker, γH2AX. NCI-H1048 cells were treated for 24h with DMSO or 300nM CIRc-004 alone or in combination with 10μM VE-821, ATR inhibitor. γH2AX and phosphorylated CHK1 were measured by Western blot. (C) Effect of Cyclin A/B RxLi on inhibition of DNA damage signaling is specific for activation of ATR versus ATM. NCI-H1048 cells were incubated with DMSO or 300nM CIRc-004 alone or in combination with 2mM hydroxyurea or 10μg/μl bleomycin for 6h, 18h or 24h. γH2AX, CHK1 and CHK2 phosphorylation were assessed by Western blot. Vinculin, loading control.

FIGURE 5. Cyclin A/B RxL inhibition impairs CHK1 phosphorylation as cells progress through S/G₂/M phase upon release from G₁



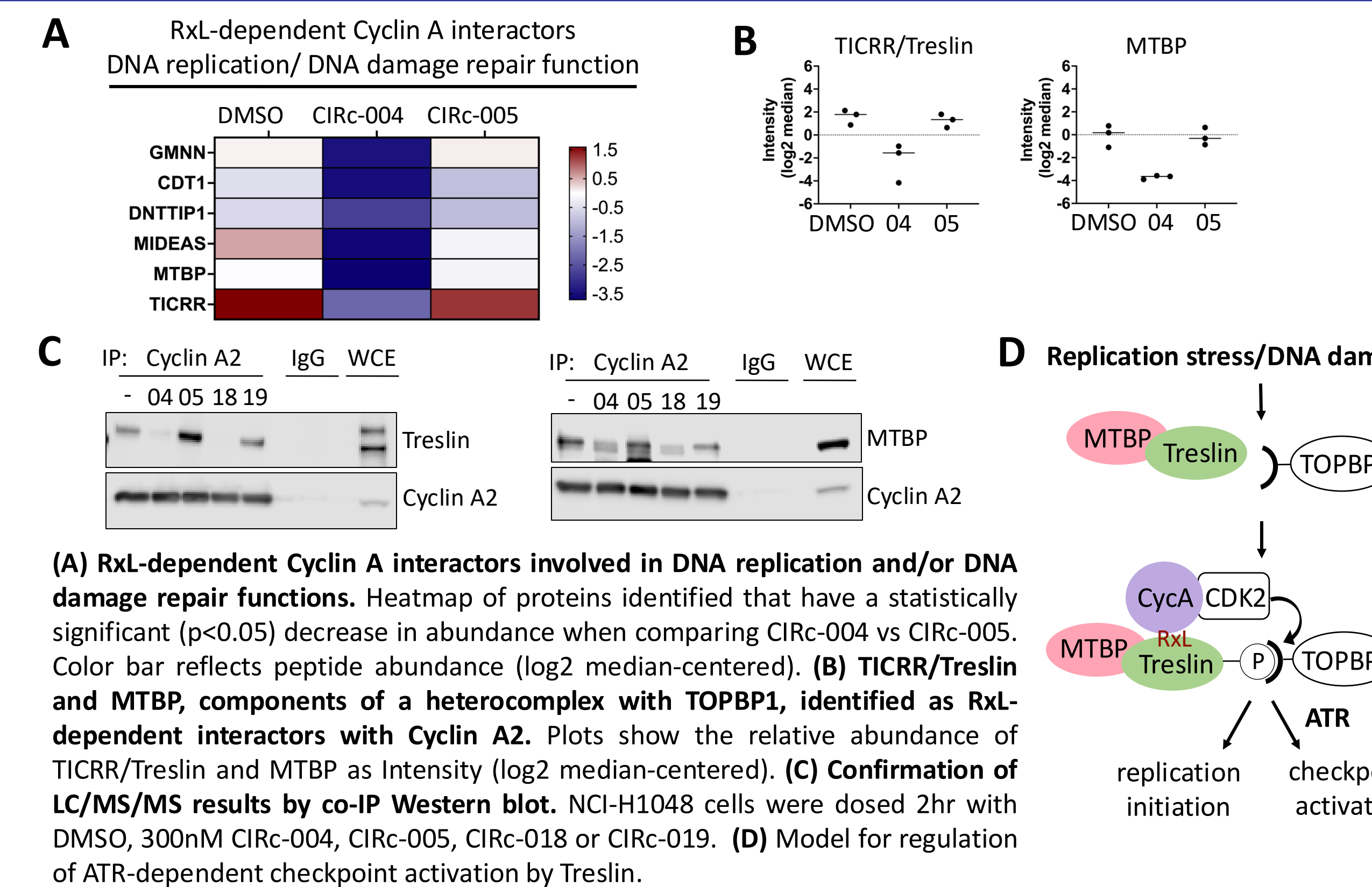
(A) Experimental schematic for NCI-H1048 double thymidine block and release (DTR). (B) Cyclin A/B RxLi does not significantly affect progression through S/G₂/M phase following DTR. NCI-H1048 were synchronized and dosed as in (A) and collected at the indicated time points for flow cytometry. 1 hr before each collection cells were pulsed with EdU. Cell cycle progression following release was assessed by detection of EdU⁺ 4N DNA content (FxCycle). (C) Cyclin A/B RxLi impairs ATR-dependent CHK1 phosphorylation during S/G₂/M phases and triggers early mitotic entry (pHH3^{S10}, 4hr post release). NCI-H1048 cells synchronized as shown in (A) were released into DMSO or 300nM CIRc-004 and collected for Western blot at the indicated times.

FIGURE 6. Identification of the Cyclin A RxL Disruptome



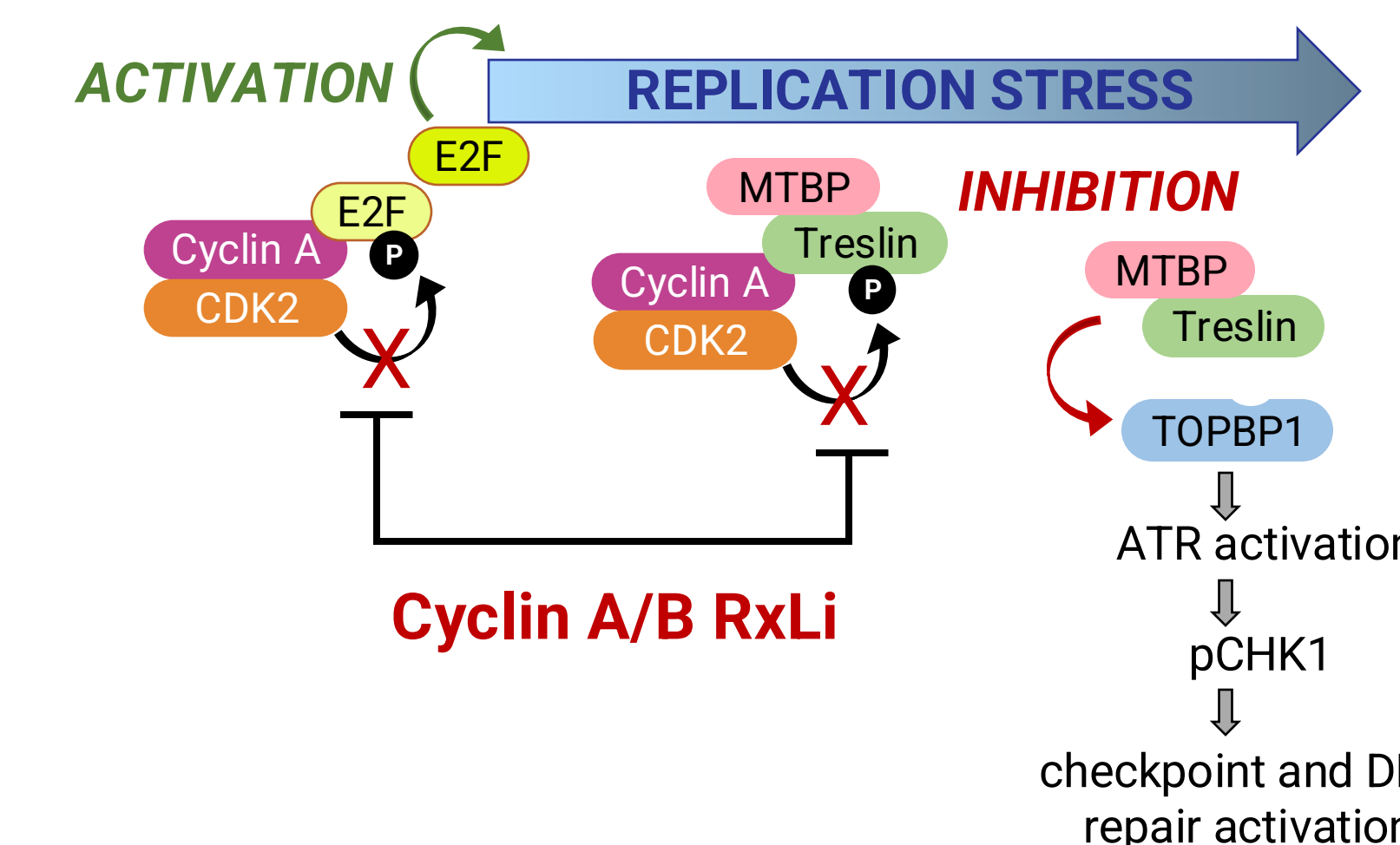
(A) Experimental schematic for identification of the Cyclin A RxL Disruptome by IP-IC/MS/MS. NCI-H1048 cells were dosed for 2hr with DMSO, 300nM CIRc-004 or CIRc-005. Cells with Cyclin A2 knock down by shRNA (CCNA2 KD) were dosed with DMSO for 2h. (B) Volcano plot comparing CIRc-004 treated cells with its inactive enantiomer, CIRc-005. 52 Cyclin A2 substrates that bind via an RxL motif were identified based on their reduced abundance in cells treated with CIRc-004 (green dots) compared to CIRc-005 (red dots). (C) Cyclin A2 disruptome identified both new and previously described RxL-dependent Cyclin A2 substrates. Plots show the relative abundance of the indicated proteins as Intensity (MaxLFQ, log₂ median-centered). Data points indicate values obtained from n=3 independent biological experiments. Examples of known RxL-dependent Cyclin A2 interactors are shown. (D) Volcano plot comparing CIRc-005 versus CCNA2 KD DMSO treated cells. Specificity of the interaction for Cyclin A2 was confirmed by increased abundance of interactors in the CIRc-005 condition (maroon dots) compared to CCNA2 KD (blue dots). (E) Cyclin A2 (bait) and CDK1/2 binding partners were pulled-down equivalently in the different treatment conditions and reduced with CCNA2 KD. Plots show the relative abundance of the indicated proteins as described in (C). (F) Intensity Ranking Plot. Ranking plot of the log₁₀ average of the 3 groups (CIRc-004, CIRc-005, DMSO) of raw protein abundance where proteins of interest are indicated within the total dataset. (G) Cyclin A2 interactome identified most of the known Cyclin A interactors listed in the String-db database. Image from Cyclin A2 protein-protein interaction network map from String-db.

FIGURE 7. TICRR/Treslin, a dual replication/DNA damage checkpoint regulator, identified as a top depleted hit



(A) RxL-dependent Cyclin A interactors involved in DNA replication and/or DNA damage repair functions. Heatmap of proteins identified that have a statistically significant (p<0.05) decrease in abundance when comparing CIRc-004 vs CIRc-005. Color bar reflects peptide abundance (log₂ median-centered). (B) TICRR/Treslin and MTBP, components of a heterocomplex with TOPBP1, identified as RxL-dependent interactors with Cyclin A2. Plots show the relative abundance of TICRR/Treslin and MTBP as Intensity (log₂ median-centered). (C) Confirmation of LC/MS/MS results by co-IP Western blot. NCI-H1048 cells were dosed 2hr with DMSO, 300nM CIRc-004, CIRc-005, CIRc-018 or CIRc-019. (D) Model for regulation of ATR-dependent checkpoint activation by Treslin.

CONCLUSIONS



- Markers of replication stress and DNA damage, including γH2AX, pRPA and a significant increase in cells with 4N DNA content undergoing DNA replication (EdU⁺ 4N), are induced by Cyclin A/B RxL inhibition in cells exposed for >6 hr, coincident with significant G₂/M accumulation.
- Cyclin A/B RxL inhibitors impair CHK1 activation by hydroxyurea but have no effect on CHK2 activation by bleomycin, suggesting a specific disruption of the ssDNA damage response signaling pathway activated by ATR.
- Using Cyclin A co-IP — LC/MS/MS in cells exposed acutely to Cyclin A/B RxLi, we have established the first Cyclin A2 RxL Disruptome, identifying many novel and previously identified Cyclin A2 substrates involved in diverse cellular functions that bind via their RxL (Cy) motif to Cyclin A.
- From the Cyclin A Disruptome, we have identified Treslin, a dual replication/checkpoint protein, and MTBP as RxL-dependent Cyclin A2 interacting partners whose interaction is disrupted by Cyclin A/B RxL inhibitors. Treslin phosphorylation by CDK2 is required for TOPBP1 binding, formation of the Treslin/MTBP/TOPBP1 heteromeric complex and phosphorylation of CHK1 (2,3,4).
- We propose that the combined effect of Cyclin A/B RxL inhibitors on E2F and Treslin/MTBP leads to an increase in replication stress/DNA damage that persists into mitosis and together with the activation of mitotic CDK by displacement of Myt1 from Cyclin B, drives the anticancer activity in E2F high SCLCs (1).

Now Enrolling CID-AB1-24001 (NCT06577987)

CID-078, Circle Pharma's clinical candidate Cyclin A/B RxL inhibitor, is currently being investigated in a phase 1 trial for patients with solid tumors including SCLC, TNBC, and tumors harboring an RB1 mutation.

Please see clinicaltrials.gov (NCT06577987) for more information.

References

- Singh S. et al. (2024) BioRxiv, currently under peer review
- Boos D. et al. (2013) Science 340, 981-984
- Kumagai A. et al. (2010) Cell 140, 349-359
- Hassan B. et al (2013) JBC 288(26), 18903-18910

